New Phytologist Supporting Information

Article title: Habitat-adapted microbial communities mediate *Sphagnum* peatmoss resilience to warming

Authors: Alyssa A. Carrell, Travis J. Lawrence, Kristine Grace M. Cabugao, Dana L. Carper, Dale A. Pelletier, Jun Hyung Lee, Sara Jawdy, Jane Grimwood, Jeremy Schmutz, Paul J. Hanson, A. Jonathan Shaw, David J. Weston

Article acceptance date: 21 February 2022

The following Supporting Information is available for this article:

Fig. S1 Average moss fluorescence in 2016 at the end of the experiment.

Fig. S2 Average moss fluorescence in 2017 at the end of the experiment.

Fig. S3 Average moss growth rate under ambient or warming treatments.

Fig. S4 Bacterial/archaeal amplicon Non-metric multidimensional scaling (NMDS) ordination of the Bray-Curtis distance matrix of inoculum and field

Fig. S5 Bacterial/archaeal amplicon Non-metric multidimensional scaling (NMDS) ordination of the Bray-Curtis distance matrix of samples at the end if the experiment.

Fig. S6 Linear correlation of plant growth rate and fungal (ITS) Shannon diversity at the conclusion of the experiment.

Fig. S7 Boxplot of percent of metatranscriptomic reads mapping to Sphagnum, metagenome assembly and metagenome assembled genomes .

Fig. S8 MDS of the top 500 most variable microbial SEED level 3 categories.

Table S1 Incubation temperature and light cycle for 2016 and 2017 laboratory experiments.

Table S2 Summary growth rate and total moss growth over 4 weeks.

Table S3 Two-way ANOVA tables of total moss growth.

Table S4 Percent change of total moss growth between microbiome transfers.

Table S5 Two-way ANOVA tables of moss fluorescence (Fv/Fm).

Table S6 Percent change of fluorescence at harvest.

Table S7 Number of paired-end bacterial/archaeal amplicon reads.

Table S8 Bacterial/archaeal amplicon-based community abundance of starting inoculum.

Table S9 Bacterial/archaeal amplicon-based community abundance at the end of lab incubations.

Table S10 Fungal amplicon (ITS) phylum level taxonomy of microbiomes at the end of the laboratory experiment.

Table S11 Fungal (ITS) class level taxonomy of microbiomes at the end of the laboratory experiment.

Table S12 Descriptive statistics and log2 fold change of metagenome assembled genomes (MAG).

Table S13 Number of paired-end metatranscriptomic reads passing quality control.

Table S14 Log2 fold change of SEED subsystem level 3 gene ontologies for the microbial fraction of metatranscriptomic reads.

Methods S1 Metagenome sequencing and analysis.

Available as separate file:

Dataset S1 Log fold change (LFC) of RNA-seq profiles from plants with ambient- and warm-microbiomes across temperature treatments.

Dataset S2 Log fold change (LFC) of RNA-seq profiles from plant-microbiomes with ambient and warming microbiomes treatments.

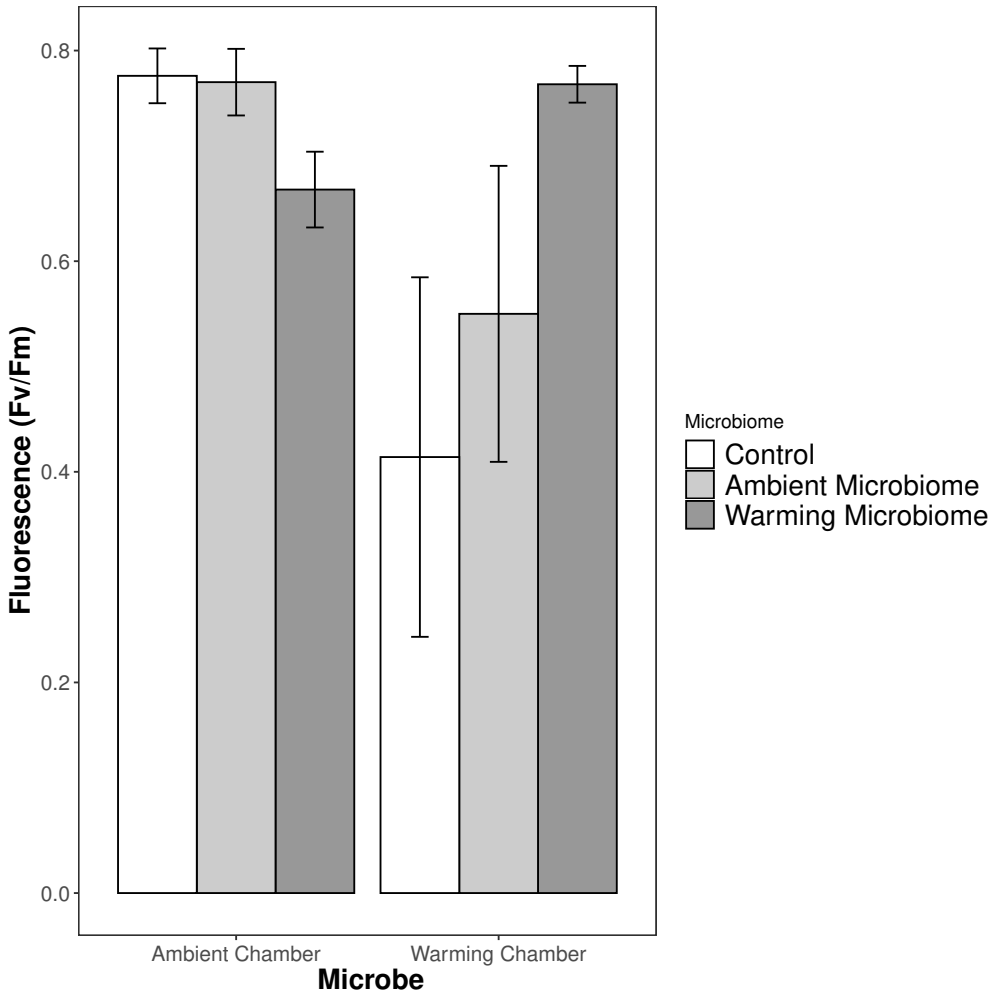

Fig. S1. Average moss fluorescence in 2016 at the end of the experiment with error bars representing standard error of the mean.

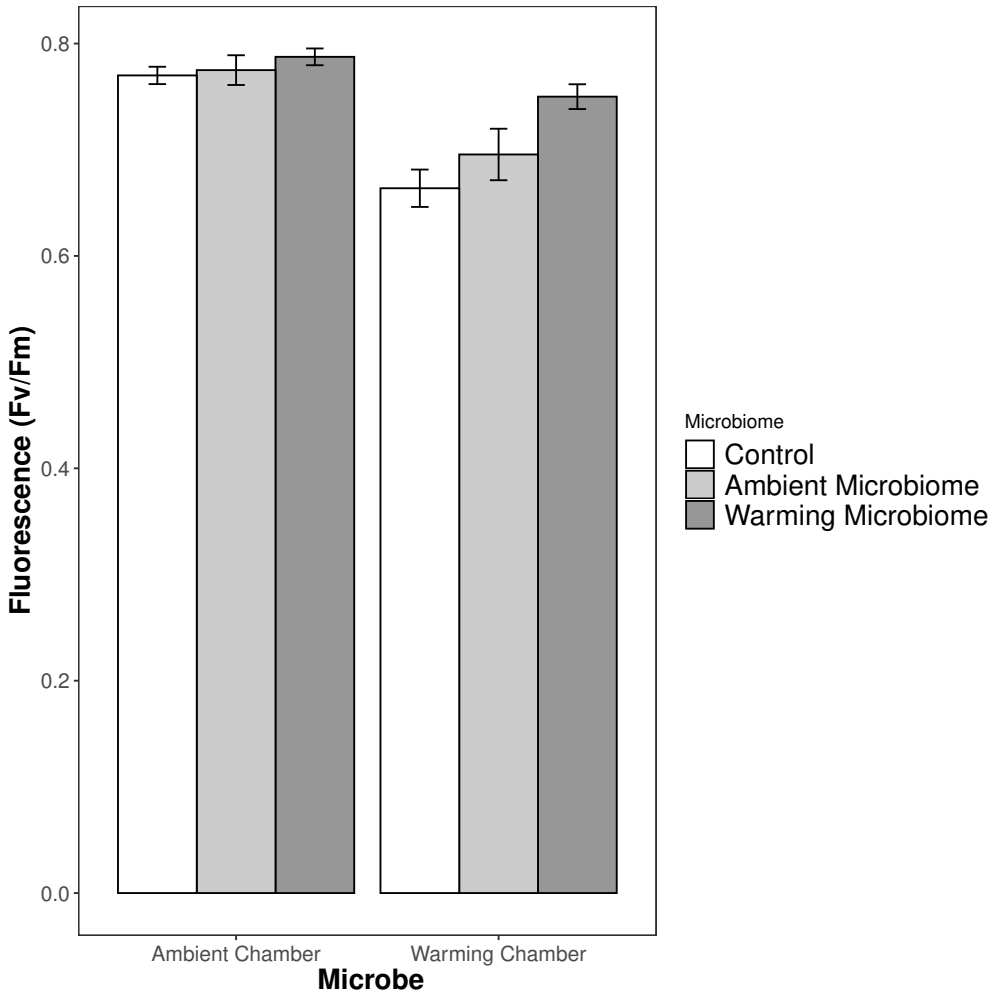

Fig. S2. Average moss fluorescence in 2017 at the end of the experiment with error bars representing standard error of the mean.

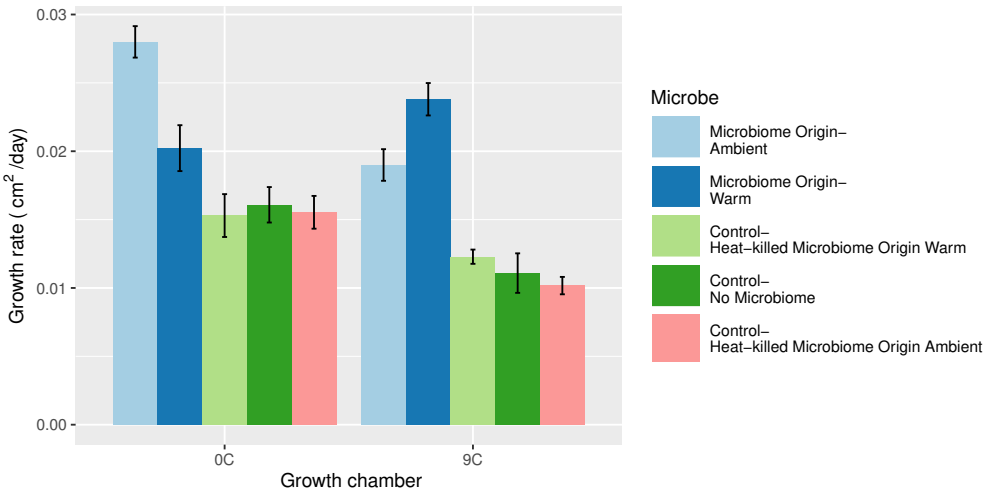

Fig. S3. Thermally conditioned intact microbiomes confer thermotolerance in host plant. No microbial controls, heat-killed controls and microbial inoculums of thermally conditioned microbiomes from glycerol stocks were applied to axenic Sphagnum before incubation in ambient or warming temperatures. Average moss growth rate under ambient or warming treatments was measured after 4 weeks. Error bars represent standard error of the mean.

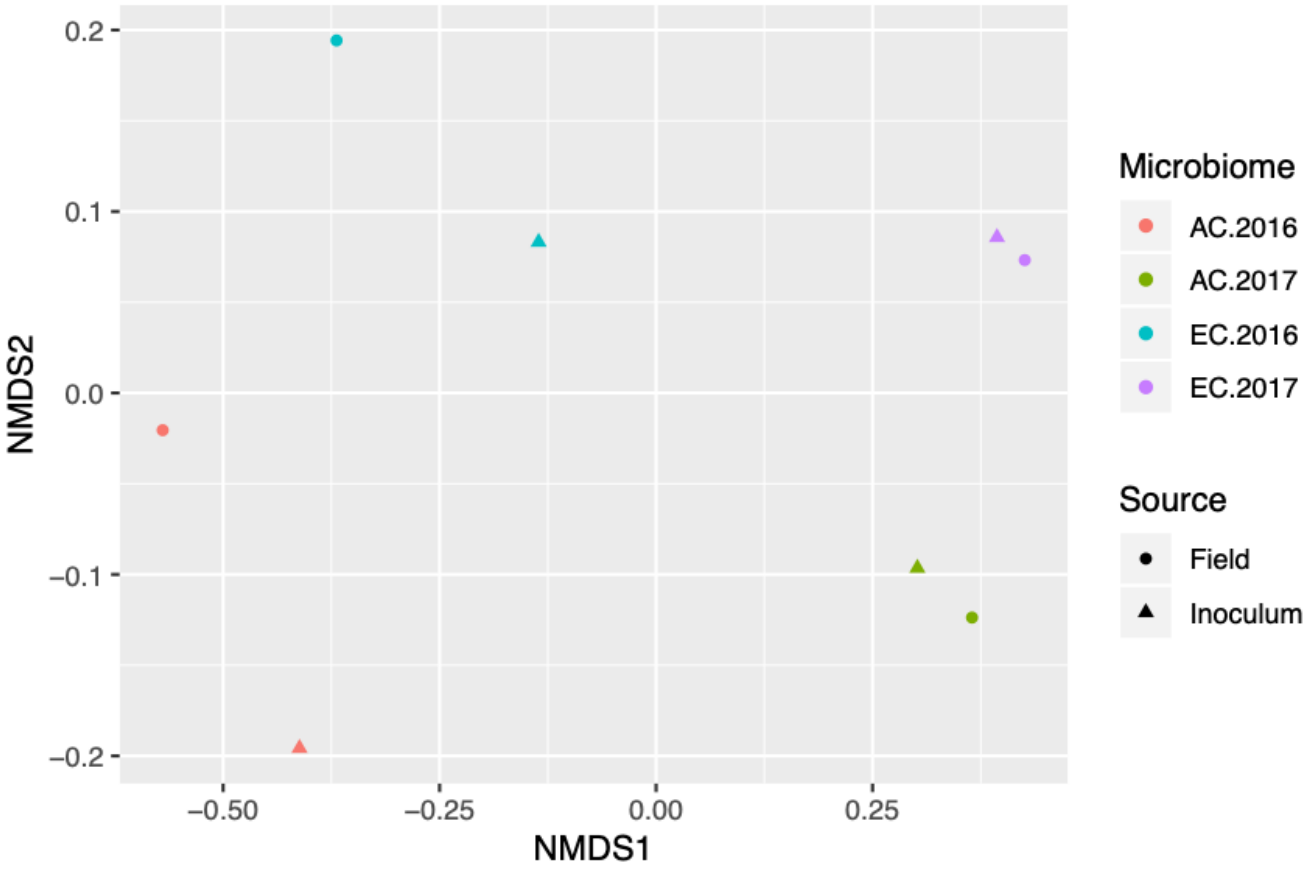

Fig. S4. Non-metric multidimensional scaling (NMDS) ordination of the Bray-Curtis distance matrix of SSU rRNA gene sequences rarefied to 19000 reads per sample. Points that are closer together on the ordination have communities that are more similar. Each point corresponds to a sample, color corresponds to the ambient (AC) and elevated (EC) SPRUCE enclosures and the year of collection, and shapes correspond to Sphagnum microbiomes from the SPRUCE site directly from field samples (field) or after the microbiomes were isolated from the field samples to be used as starting inoculum for incubation experiments in the laboratory.

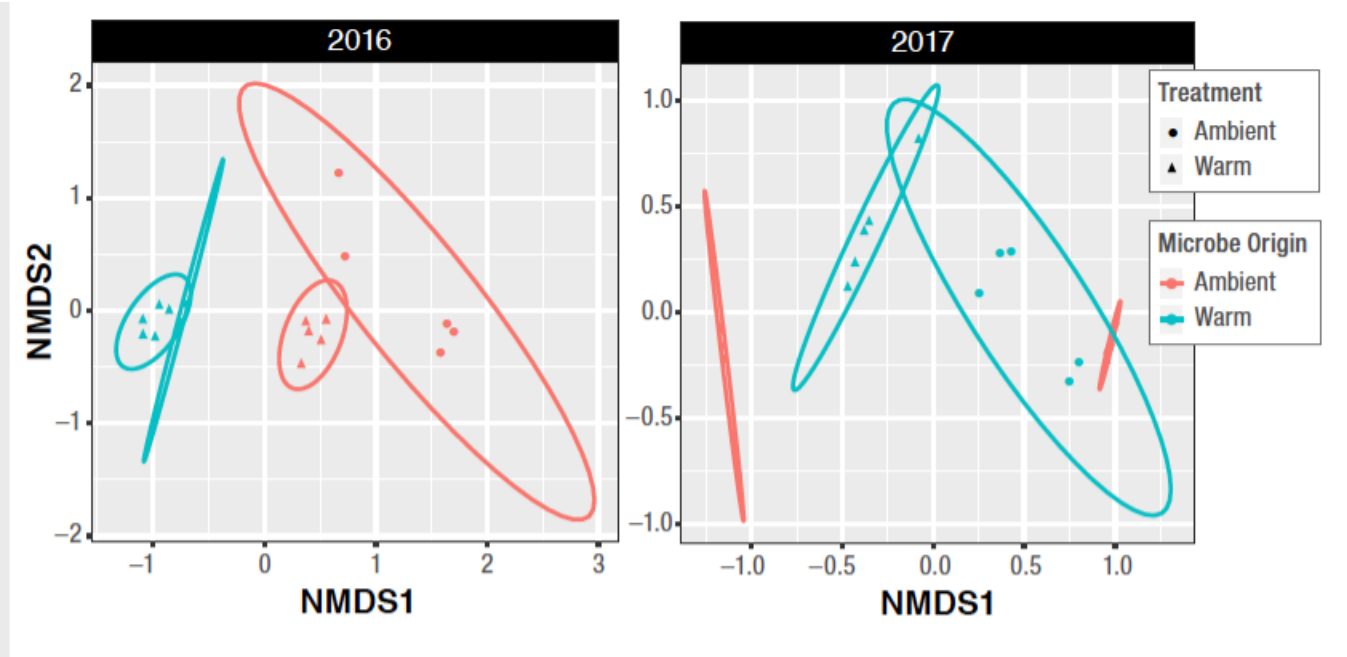

Fig. S5. Non-metric multidimensional scaling (NMDS) ordination of the microbiome Bray-Curtis distance matrix. Points that are closer together on the ordination have communities that are more similar. Each point corresponds to a sample, color corresponds to the microbiome thermal origin from ambient and warm field plots. Shapes correspond to the chamber that axenic plants were incubated at ambient or warm temperatures.

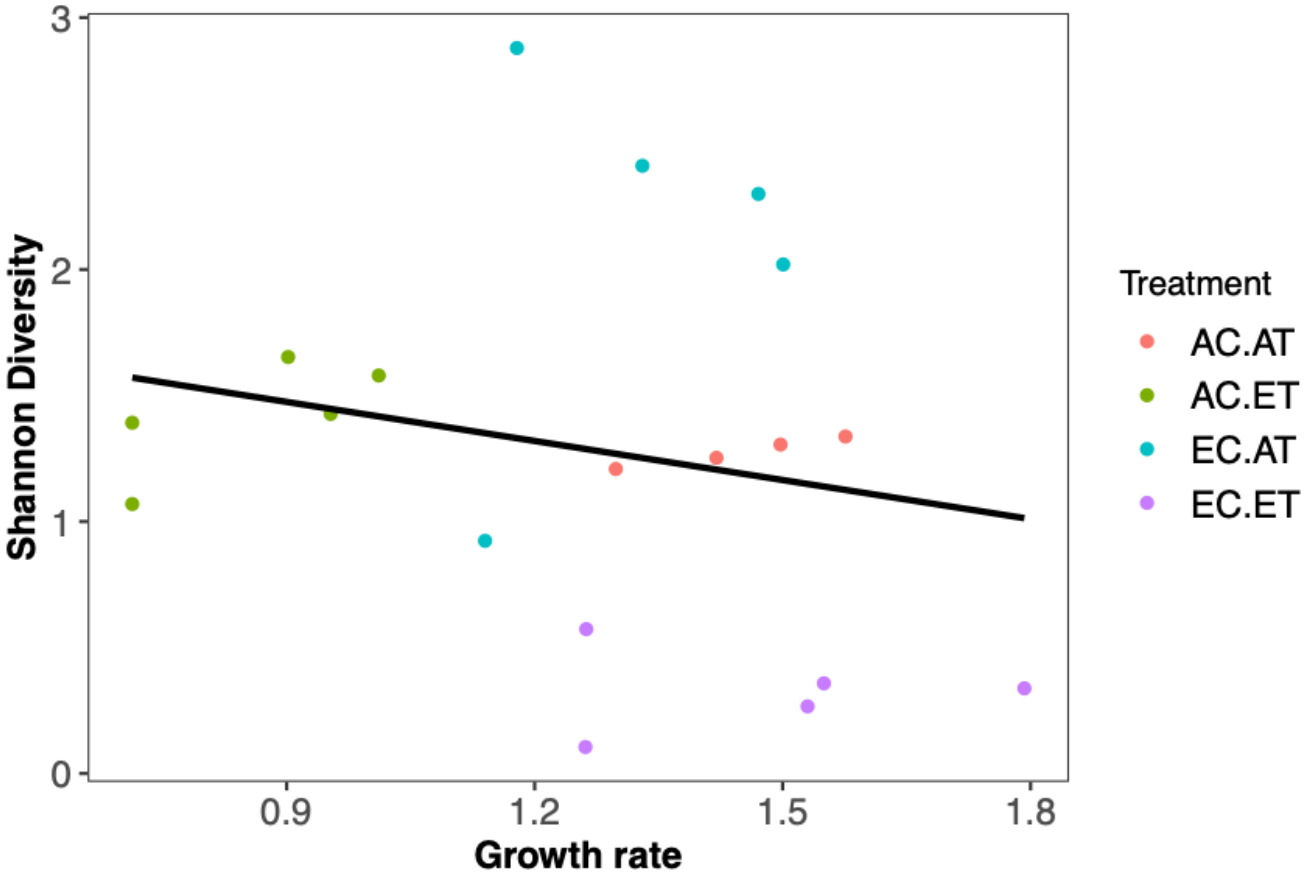

Fig. S6. Linear correlation of plant growth rate and fungal (ITS) Shannon diversity at the conclusion of the experiment. Each point corresponds to a sample with colors indicating ambient chamber/ambient microbiome (AC.AT), ambient chamber/warming microbiome (EC.AT), warming chamber/ambient microbiome (AC.ET), or warming chamber/warming microbiome (EC.ET).

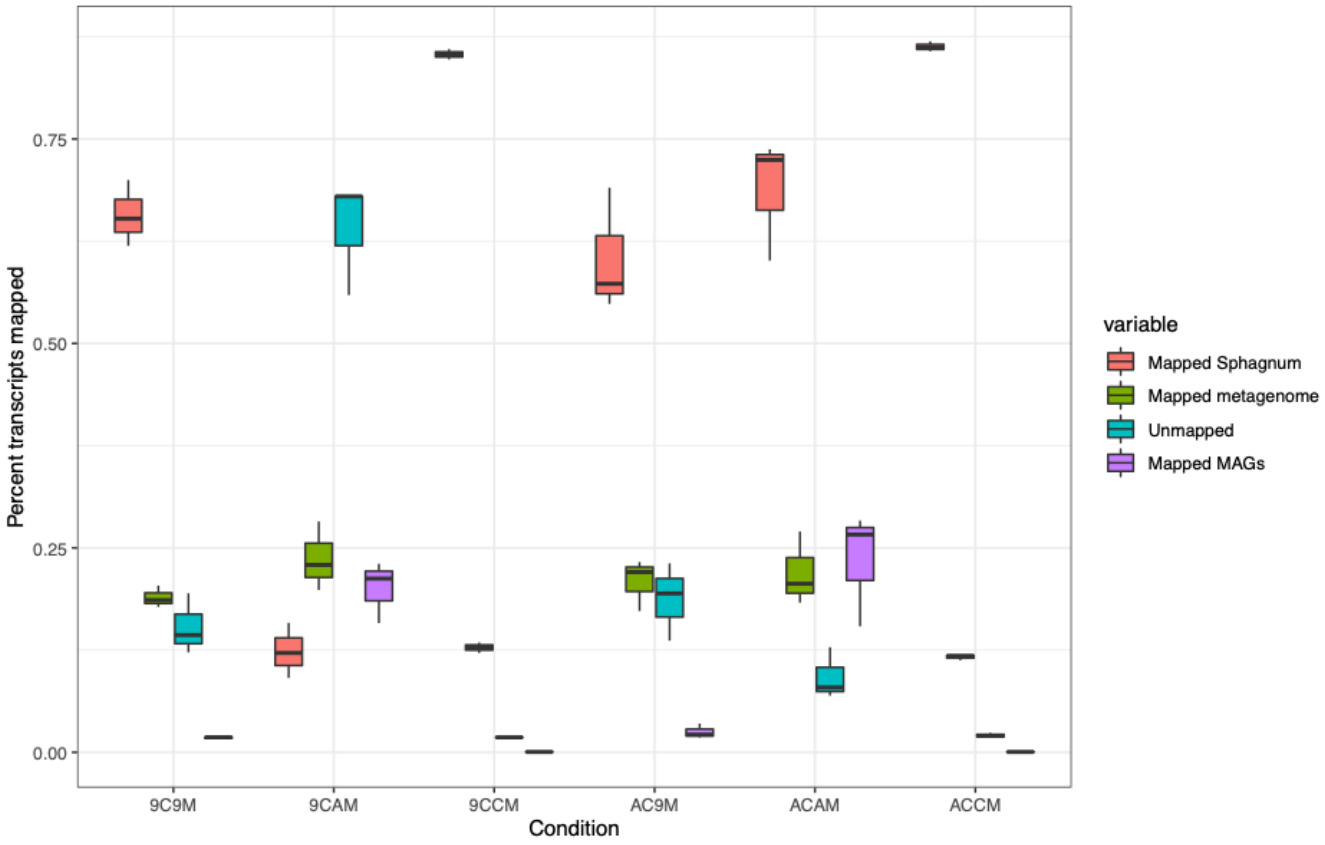

Fig. S7. Boxplot of percent of metatranscriptomic reads mapping to Sphagnum fallax (red), metagenome assembly, and metagenome assembled genomes (purple), or not mapping (blue) for ambient chamber/ambient microbiome (ACAM), ambient chamber/warming microbiome (AC9M), warming chamber/ambient microbiome (9CAM), warming chamber/warming microbiome (9C9M), ambient chamber/no microbiome addition (ACCM), and warming chamber/no microbiome addition (9CCM). Boxes span from the first to the third quartile, black bar indicates median, and whiskers span 1.5 * interquartile range.

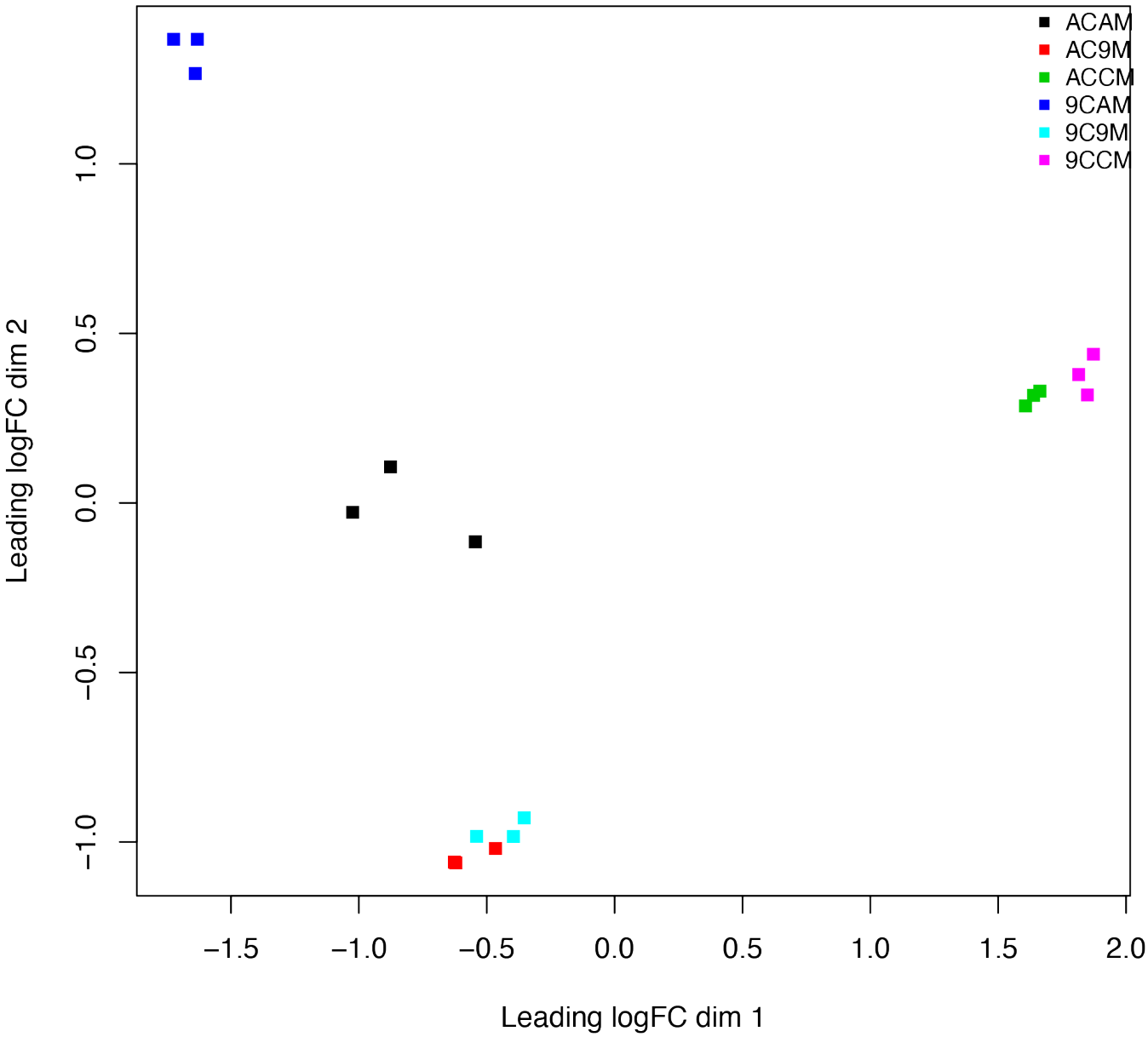

Fig. S8. MDS based on the top 500 most variable SEED level 3 categories of the microbial partition of the metatranscriptome. Abbreviations are defined in Fig. S6

Table S1. Incubation temperature and light cycle for 2016 and 2017 laboratory experiments. Temperatures were determined from June 2016 average temperature for 6 hour blocks at the SPRUCE site.

Treatment Chamber	Time	Temperature (C)	Light
Ambient +0C	0:00	13	No
	6:00	18	Yes
	12:00	21	Yes
	18:00	15	No
Ambient +9C	0:00	22	No
	6:00	27	Yes
	12:00	30	Yes
	18:00	24	No

Table S2. Summary growth rate and total moss growth over 4 weeks.

Year	Chamber	Microbiome origin	N	Mean growth rate (mm/day)	SD growth rate	SE growth rate	Mean growth (mm)	SD growth	SE growth
2016	Ambient	Ambient	6	1.664	0.448	0.200	46.601	12.534	5.605
	Ambient	Control	6	1.060	0.718	0.321	29.687	20.104	8.991
	Ambient	Warming	6	1.098	0.786	0.352	30.736	22.017	9.846
	Warming	Ambient	6	0.887	0.569	0.255	24.849	15.936	7.127
	Warming	Control	6	0.202	0.202	0.090	5.645	5.645	2.525
	Warming	Warming	6	1.759	0.418	0.187	49.251	11.692	5.229
2017	Ambient	Ambient	12	1.407	0.288	0.083	29.548	6.057	1.749
	Ambient	Control	12	1.088	0.117	0.034	22.844	2.455	0.709
	Ambient	Warming	12	1.311	0.186	0.054	27.537	3.906	1.128
	Warming	Ambient	12	0.593	0.455	0.131	12.455	9.564	2.761
	Warming	Control	12	0.188	0.179	0.052	3.948	3.758	1.085
	Warming	Warming	12	1.460	0.170	0.049	30.662	3.563	1.028

Table S3. Two-way ANOVA tables of total moss growth. Data were ranked transformed prior to analysis. Chamber refers to the experimental temperature treatment.

	Sum of Squares	DF	F-value	P-value
2016				
Intercept	2420.00	1	53.226	<0.05
Chamber	211.60	1	4.654	<0.05
Microbe	170.53	2	1.875	0.175
Chamber:Microbiome	516.47	2	5.680	<0.05
Residuals	1091.20	24		
2017				
Intercept	32865	1	308.448	<0.05
Chamber	7633	1	71.634	<0.05
Microbe	2477	2	11.621	<0.05
Chamber:Microbiome	6823	2	32.016	<0.05
Residuals	7032	66		

Table S4. Percent change of total moss growth between microbiome transfers relative to moss without a microbiome within the same chamber calculated as: (treatment microbiome − no microbiome)/no microbiome. Non-significant comparisons are indicated with 'ns'.

Year	Chamber	Microbiome	Percent change	p-value
2016	Ambient	Ambient	36%	ns
	Ambient	Warming	3%	ns
	Warming	Ambient	77%	ns
	Warming	Warming	89%	<0.05
2017	Ambient	Ambient	23%	<0.05
	Ambient	Warming	17%	<0.05
	Warming	Ambient	68%	ns
	Warming	Warming	87%	<0.05

Table S5. Two-way ANOVA tables of moss fluorescence (Fv/Fm). Data were ranked transformed prior to analysis. Chamber refers to the experimental temperature treatment.

	Sum of squares	DF	F-value	P-value
2016				
Intercept	2000.00	1	37.433	<0.05
Chamber	225.62	1	4.223	0.051
Microbe	352.43	2	3.298	0.054
Chamber:Microbiome	822.02	2	7.693	<0.05
Residuals	1282.30	24		
2017				
Intercept	17328.0	1	40.135	<0.05
Chamber	222.0	1	0.514	0.476
Microbe-Origin	577.8	2	0.669	0.516
Chamber:Microbiome	328.8	2	0.381	0.685
Residuals	28494.8	66		

Table S6. Percent change of fluorescence at harvest between microbiome transfers relative to moss without a microbiome within the same chamber calculated as: $(\textbf{treatment microbiome} - \textbf{no microbiome})/\textbf{no microbiome}$. Non-significant comparisons are indicated with 'ns'.

Year	Chamber	Microbiome	Percent change	p-value
2016	Ambient	Ambient	-0.78%	ns
	Ambient	Warming	-16.17%	ns
	Warming	Ambient	24.73%	ns
	Warming	Warming	46.09%	ns
2017	Ambient	Ambient	0.65%	ns
	Ambient	Warming	2.28%	ns
	Warming	Ambient	4.59%	ns
	Warming	Warming	11.47%	ns

Table S7. Number of paired-end amplicon reads after quality filtering and removal of plastid DNA.

Year	Chamber	Microbiome	Rep	Read
2016	Ambient	Ambient	1	28141
			2	25327
			3	19666
			4	55905
			5	40527
	Ambient	Warming	1	27700
			2	36244
			3	53569
			4	45765
			5	48325
	Warming	Ambient	1	42631
			2	31655
			3	67278
			4	40788
			5	83227
	Warming	Warming	1	48319
			2	41081
			3	42373
			4	84018
			5	23128
2017	Ambient	Ambient	1	165122
			2	97861
			3	109430
			4	73358
			5	74235
	Ambient	Warming	1	229026
			2	111912
			3	187135
			4	202455
			5	173016
	Warming	Ambient	1	98447
			2	95805
			3	95300
			4	92978
			5	142548
	Warming	Warming	1	90474
			2	95494
			3	150805
			4	120406
			5	62401

Table S8. Bacterial/archaeal amplicon-based community abundance table for starting inoculums isolated from the ambient (AC) and warming (EC) SPRUCE enclosures and the year of collection. Bacterial classes not detected in samples are indicated with 'NA'.

Class	AC.2016	AC.2017	EC.2016	EC.2017
c__[Fimbriimonadia]	NA	0.0048	NA	0.0044
c__[Methylacidiphilae]	0.0067	0.0422	NA	0.0175
c__[Pedosphaerae]	0.017	0.0644	0.0059	0.0463
c__[Saprospirae]	0.0227	0.0447	0.0441	0.0329
c__[Spartobacteria]	0.0044	0.0303	0.0011	0.018
c__4C0d-2	0.0015	0.0058	NA	0.0026
c__Acidimicrobiia	0.0049	0.0065	NA	0.0066
c__Acidobacteriia	0.124	0.1127	0.0641	0.1329
c__Actinobacteria	0.0168	0.0093	0.0039	0.0035
c__Alphaproteobacteria	0.3211	0.2954	0.0805	0.3033
c__Armatimonadia	NA	0.0031	NA	0.0033
c__Bacilli	NA	NA	0.0151	NA
c__Bacteroidia	0.008	NA	0.0016	NA
c__Betaproteobacteria	0.0642	0.0562	0.1706	0.0803
c__Chlamydiia	0.0141	0.0082	0.0047	0.0107
c__Chthonomonadetes	NA	0.0031	NA	0.0061
c__Clostridia	0.1609	NA	0.0654	NA
c__Coriobacteriia	0.0018	NA	NA	NA
c__Cytophagia	NA	0.0018	NA	0.0047
c__Deltaproteobacteria	0.0057	0.0272	0.0014	0.0192
c__Elusimicrobia	0.0018	0.0014	NA	0.0015
c__Flavobacteriia	NA	NA	0.0013	0.0014
c__Gammaproteobacteria	0.103	0.1115	0.4248	0.1448
c__Holophagae	NA	NA	0.0259	NA
c__Methanobacteria	0.0421	NA	0.0088	NA
c__Methanomicrobia	0.0014	NA	NA	NA
c__Nostocophycideae	0.0053	0.0189	NA	0.0173
c__Opitutae	0.0111	0.0127	0.0019	0.0087
c__Phycisphaerae	0.0037	0.0232	NA	0.015
c__Planctomycetia	0.0076	0.02	NA	0.0233
c__SBRH58	NA	0.001	NA	NA
c__SJA-4	0.0011	0.0022	NA	0.0011
c__Solibacteres	0.0109	0.0237	NA	0.047
c__Sphingobacteriia	0.0267	0.0531	0.0722	0.0377
c__Thermoleophilia	0.0025	0.0048	NA	0.0027
c__Thermoplasmata	0.0019	NA	NA	NA
c__TM7-1	NA	0.0016	NA	NA
c__vadinHA49	NA	0.0017	NA	NA
c__Verrucomicrobiae	NA	0.002	NA	0.0013
c__ZB2	NA	0.0011	NA	NA
Other	0.007	0.0054	0.0066	0.0062

Table S9. Bacterial/archaeal amplicon-based community abundance table for samples at the end of the experiment for the ambient chamber/ambient microbiome (AC.AT), ambient chamber/warming microbiome (EC.AT), warming chamber/ambient microbiome (AC.ET), and warming chamber/warming microbiome (EC.ET). Bacterial classes not detected in samples are indicated with 'NA'.

Year	2016				2017			
Class	AC.AT	AC.ET	EC.AT	EC.ET	AC.AT	AC.ET	EC.AT	EC.ET
c__[Methylacidiphilae]	NA	NA	0.024	NA	0.028	NA	NA	NA
c__[Pedosphaerae]	0.083	0.025	0.032	0.024	0.043	NA	NA	NA
c__[Saprospirae]	0.024	0.094	0.083	NA	0.071	0.261	0.316	0.19
c__[Spartobacteria]	0.026	0.211	0.086	NA	0.053	NA	NA	0.026
c__Acidobacteriia	0.089	0.066	0.104	0.055	0.074	NA	NA	NA
c__Actinobacteria	NA	NA	NA	NA	0.026	NA	NA	NA
c__Alphaproteobacteria	0.288	0.189	0.185	0.221	0.256	0.146	0.159	0.258
c__Betaproteobacteria	0.111	0.202	0.229	0.339	0.105	0.049	0.153	0.116
c__Clostridia	0.089	NA	NA	0.119	NA	NA	NA	NA
c__Deltaproteobacteria	NA	NA	NA	NA	0.021	NA	0.036	0.021
c__Flavobacteriia	NA	NA	NA	NA	NA	0.07	0.074	NA
c__Gammaproteobacteria	0.091	0.046	0.059	0.052	0.071	NA	0.034	0.097
c__Methanobacteria	0.023	NA	NA	0.03	NA	NA	NA	NA
c__Nostocophycideae	NA	NA	NA	NA	0.136	NA	NA	NA
c__Opitutae	0.027	NA	NA	NA	NA	NA	NA	0.054
c__SJA-4	NA	NA	NA	NA	0.024	NA	NA	NA
c__Solibacteres	NA	0.029	0.021	NA	NA	NA	NA	0.063
c__Sphingobacteriia	NA	NA	0.036	0.03	0.029	NA	NA	0.069
c__Synechococcophycideae	NA	NA	NA	NA	NA	0.419	0.133	NA
c__Verrucomicrobiae	NA	0.04	0.057	NA	NA	NA	0.026	NA
Other	0.149	0.097	0.084	0.13	0.064	0.056	0.07	0.107

Table S10. Fungal amplicon (ITS) phylum level taxonomy of microbiomes at the end of the laboratory experiment. Column headings are defined in table S9.

Phylum	AC.AT	AC.ET	EC.AT	EC.ET
Ascomycota	1.00	1.00	0.99	1.00
Other	0.00	0.00	0.01	0.00

Table S11. Fungal (ITS) class level taxonomy of microbiomes at the end of the laboratory experiment. Column headings are defined in table S9. Fungal classes not detected in samples are indicated with 'NA'.

Class	AC.AT	AC.ET	EC.AT	EC.ET
Dothideomycetes	0.06	0.03	0.31	NA
Leotiomycetes	0.93	0.26	0.47	0.99
Sordariomycetes	NA	0.71	0.20	NA
Other	0.01	0.00	0.03	0.01

Table S12. Descriptive statistics and log2 fold change of metagenome assembled genomes (MAG). Marker lineage, completeness, contamination, and strain heterogeneity were calculated using checkM. Log2 fold change between warming and ambient metagenomic samples were determined by mapping reads metagenomic reads back to MAGs using BAMM and calculating counts per million mapped reads.

Bin Id	Marker lineage	Completeness	Contamination	Strain heterogeneity	Warm reads/million	Ambient reads/million	log2FC (warm/ambient)
bin.354	p__Cyanobacteria (UID2189)	98.22	0	0	2478.68	0.27	13.18
bin.259	k__Bacteria (UID2982)	97.97	0.68	0	0.45	1420.09	-11.61
bin.156	p__Bacteroidetes (UID2605)	94.77	0.27	66.67	0.55	818.74	-10.53
bin.104	p__Bacteroidetes (UID2605)	92.42	2.1	10	3.33	1210.89	-8.51
bin.192	p__Cyanobacteria (UID2193)	88.92	0.84	0	1674.53	5.91	8.15
bin.99	o__Burkholderiales (UID4000)	98.3	2.1	18.18	1165.13	8.18	7.15
bin.287	k__Bacteria (UID2982)	88.68	0.68	0	312.60	3.67	6.41
bin.23	k__Bacteria (UID3187)	93.41	3.42	28.57	71.84	3560.88	-5.63
bin.15	p__Bacteroidetes (UID2605)	93.79	2.94	33.33	1844.19	37.42	5.62
bin.184	k__Bacteria (UID3187)	83.1	1.71	50	695.57	14.82	5.55
bin.56	k__Bacteria (UID3187)	91.64	4	42.86	35.34	1541.88	-5.45
bin.309	o__Burkholderiales (UID4002)	96.81	2.12	55.56	72.21	2529.74	-5.13
bin.47	k__Bacteria (UID3187)	90.8	3.45	20	42.94	1476.55	-5.10
bin.81	k__Bacteria (UID203)	73.28	2.59	100	86.65	2811.99	-5.02
bin.292	k__Bacteria (UID203)	75	1.72	100	21.23	648.77	-4.93
bin.17	o__Rhodospirillales (UID3754)	94.96	1.62	50	144.65	3359.09	-4.54
bin.121	c__Alphaproteobacteria (UID3422)	94.64	5	13.64	57.94	1116.78	-4.27
bin.167	f__Bradyrhizobiaceae (UID3695)	93.76	3.89	40.91	336.88	3913.99	-3.54
bin.313	o__Burkholderiales (UID4000)	78.47	2.66	38.46	629.98	61.81	3.35
bin.59	k__Bacteria (UID2982)	94.59	0.68	0	59.45	509.63	-3.10
bin.298	k__Bacteria (UID2982)	70.78	1.91	0	173.80	22.14	2.97
bin.229	o__Rhodospirillales (UID3754)	92.89	3.69	52.94	123.26	929.91	-2.92
bin.72	p__Bacteroidetes (UID2591)	77.35	1.48	0	520.27	70.11	2.89
bin.14	p__Cyanobacteria (UID2189)	99	0.63	0	399.29	2790.31	-2.80
bin.79	o__Rhizobiales (UID3654)	84.7	3.33	57.14	604.69	92.00	2.72
bin.221	o__Rhizobiales (UID3654)	97.44	4.23	70.59	155.60	958.54	-2.62
bin.33	c__Gammaproteobacteria (UID4202)	89.23	4.73	38.1	483.01	2753.98	-2.51
bin.120	c__Betaproteobacteria (UID3888)	88.46	1.33	0	208.76	1131.76	-2.44
bin.208	o__Rhodospirillales (UID3754)	76.88	2.99	77.78	1000.52	204.32	2.29
bin.326	k__Bacteria (UID2982)	99.27	4.26	40	1456.93	320.12	2.19
bin.31	k__Bacteria (UID203)	80.17	0	0	2016.91	8598.72	-2.09
bin.302	o__Rhodospirillales (UID3754)	98.64	4.34	71.43	1493.89	556.02	1.43
bin.255	p__Bacteroidetes (UID2591)	86.59	2.73	11.11	260.69	503.76	-0.95
bin.189	o__Rhodospirillales (UID3754)	95.32	3.24	45.45	705.99	1259.43	-0.84
bin.265	k__Bacteria (UID1453)	97.29	3.99	0	580.23	1011.39	-0.80
bin.286	c__Alphaproteobacteria (UID3305)	93.01	1.02	33.33	387.08	234.46	0.72
bin.247	c__Gammaproteobacteria (UID4202)	96.46	3.83	33.33	629.26	964.26	-0.62
bin.243	k__Bacteria (UID2982)	93.68	0.68	0	881.61	603.55	0.55
bin.202	o__Rhodospirillales (UID3754)	92.42	0.72	33.33	688.67	501.22	0.46
bin.289	k__Bacteria (UID2495)	83.15	1.12	100	294.65	219.73	0.42
bin.92	o__Rhodospirillales (UID3754)	99.1	1.41	20	1088.07	920.00	0.24
bin.257	k__Bacteria (UID2982)	85.62	6.4	37.5	1098.88	958.34	0.20
bin.339	k__Bacteria (UID3187)	88.7	2.78	42.86	1750.25	1985.11	-0.18
bin.132	p__Bacteroidetes (UID2605)	93.04	3.25	55.56	686.18	613.76	0.16
bin.223	o__Rhodospirillales (UID3754)	92.83	4.81	7.69	550.96	579.56	-0.07
bin.198	o__Actinomycetales (UID1593)	98.48	2.27	40	624.26	609.67	0.03

Table S13. Number of paired-end metatranscriptomic reads passing quality control. Quality trimming was performed at the Q20 level and if either read of a pair was <75 bp after adapter removal and quality trimming the read pair was discarded.

Chamber	Microbiome	Rep	Counts of paired-end reads passing QC	Plant Reads	Bacterial/Archaeal reads	Fungal Reads
	Ambient	1	49,339,226	35524243	8880173	887
Ambient	Ambient	2	35,987,608	20872813	8995462	1431
	Ambient	3	39,865,568	25513964	10363804	1245
	Warming	1	33,372,123	20690716	7674667	1021
Ambient	Warming	2	31,528,203	23015588	6620128	788
	Warming	3	41,055,820	25044050	8210179	991
	Control	1	29,530,155	25395933	3543193	433
Ambient	Control	2	37,222,244	31638907	4838311	582
	Control	3	31,634,008	27205247	4111928	483
	Ambient	1	56,084,411	5608441	8379011	1716199
Warming	Ambient	2	48,673,151	7300973	8620015	2574810
	Ambient	3	42,032,880	4623617	11008411	340461
	Warming	1	46,801,800	31825224	6083504	733
Warming	Warming	2	35,071,333	18587806	4909397	589
	Warming	3	41,731,001	24203981	5424379	661
	Control	1	45,655,644	39263854	5660621	683
Warming	Control	2	49,482,126	42059807	5991566	719
	Control	3	41,676,823	35842068	5000619	605
			Total	**60.29%**	**16.87%**	**0.63%**

Table S14. Log2 fold change of SEED subsystem level 3 gene ontologies for the microbial fraction of metatranscriptomic reads. Read mapping and feature counts were determined using the SAMSA pipeline and differential expression analysis was performed with limma-voom. Abbreviations are defined as ambient chamber/ambient temperature conditioned microbiome (ACAM), +9C chamber/ambient temperature conditioned microbiome (9CAM), Ambient chamber/+9C temperature conditioned microbiome (AC9M), +9C chamber/+9C temperature conditioned microbiome (9C9M) and, avg(9M) which indicates the average of 9C9M and AC9M. Non-significant comparisons are indicated with 'ns'.

SEED L3 Classification	log2(9CAM/ACAM)	log2(9C9M/AC9M)	log2(avg(9M)/ACAM)
Nitrogen Metabolism			
Allantoin Utilization	-2.43	NS	NS
Amidase clustered	-1.73	NS	-1.14
Ammonia assimilation	2.78	NS	NS
Nitrate/nitrite ammonification	2.62	NS	NS
Nitric_oxide_synthase	-1.55	NS	NS
Nitrogen_fixation	-5.74	NS	-7.99
Nitrosative_stress	1.85	NS	NS
Heterocyst cyanobacteria	-2.01	-1.64	-8.64
Sulfur Metabolism			
Sulfur_oxidation	2.91	NS	2.27
Taurine_Utilization	NS	NS	1.70
Glutathione as Sulphur source	1.69	NS	2.51
Galactosylceramid/Sulfatide_metabolism	-2.55	NS	NS
Inorganic_Sulfur_Assimilation	1.03	NS	NS
Stress			
Universal_stress_protein_family	2.41	NS	-1.70
GroEL_GroES	1.39	NS	NS
Heat_shock_dnaK_gene_cluster	1.50	NS	NS
Photo/Cyano			
Cyanobacterial_Circadian_Clock	1.03	NS	-4.39
Myxoxanthophyll biosynthesis Cyanobacteria	1.72	2.54	-7.55
Bacterial_light-harvesting_protein	NS	4.42	NS
Bacteriorhodopsin	-1.05	NS	NS
PSII-type reaction_center	-1.31	2.85	NS
Photosystem_I	1.84	NS	NS
Photosystem_II	1.11	NS	NS
Phycobilisome	1.75	NS	-8.89
One Carbon Metabolism			
Formaldehyde_assimilation:_Ribulose_monophosphate_pathway	-1.24	NS	NS
One-carbon_metabolism_by_tetrahydropterines	NS	NS	1.98
Serine-glyoxylate_cycle	NS	NS	NS
Soluble_methane_monooxygenase	-2.66	NS	NS

Methods S1: Metagenome and sequence analysis Metagenomics of the starting inoculum

DNA for metagenomics was extracted using a modified CTAB method (Carrell & Frank, 2014). The ambient- and warming-conditioned microbiome samples were sequenced as an Illumina TruSeq PCR-Free library on an Illumina 2500 in Rapid Run mode (paired-end, 2 × 150 nt). Raw sequences were processed using Atropos v. 1.1.17 (Didion *et al.*, 2017) in Python v3.6.2 to remove adapter contamination and quality trimming. Quality trimming was performed at the Q20 level with read pairs, and if either read of a pair was < 75 bp after adapter removal and quality trimming, the read pair was discarded. Before metagenome assembly, we removed reads mapping to either the *S. angustifolium* or PhiX genomes using bbmap v38.22. The remaining metagenome reads for the ambient and warming samples were co-assembled using MEGAHIT v1.1.3 (Li *et al.*, 2015, 2016) with default settings except --min-contig-len was set to 300. Trimmed paired-end reads were mapped to the MEGAHIT co-assembly with BamM v1.7.3 (http://ecogenomics.github.io/BamM/) (Li & Durbin, 2009). Putative genomes were binned from the co-assembled contigs using MetaBAT v2.12.1 (Kang *et al.*, 2019) with –minContig set to 2000. Metagenome-assembled genomes (MAGs) were assessed for completeness, contamination, and strain contamination using checkM v1.0.12 (Parks *et al.*, 2015). MAGs that were ³ 70% complete with £ 5% contamination were kept for downstream analyses. To determine differences in the relative abundance of MAGs between ambient and warming metagenome samples, trimmed metagenomic reads were mapped to MAGs using BamM v.1.7.3 and normalized as counts per million mapped reads. Gene models were predicted for the co-assembled metagenomic contigs using Prodigal v2.6.3 (Hyatt *et al.*, 2010) in anonymous mode, and MAGs were annotated using prokka v1.14.0 (Seemann, 2014). Taxonomy was assigned to gene models using the lowest common ancestor algorithm implemented in DIAMOND v0.9.22 (Buchfink *et al.*, 2014). Inferred amino acid sequences were searched against the NCBI non-redundant protein database (downloaded October 3, 2019) using default settings in DIAMOND BLASTp except as follows: --query-cover 85, --top 5, and --sensitive.

Phylogenetic analysis of cyanobacterial MAGs

We downloaded 109 cyanobacterial RefSeq genomes from NCBI representing the currently sequenced diversity of clade A (*Oscillatoria*/*Arthrospira*) and clade B (*Nostoc*/*Anabaena*/*Cyanothece*), following the nomenclature of (Shih *et al.*, 2013), and two outgroup taxa, *Acaryochloris* sp. CCMEE 5410 and *A. marina* MBIC11017. Additionally, we included six cyanobacterial isolates sequenced in (Warshan *et al.*, 2017), *Nostoc moss6*, *N. moss3*, *N. moss2*, *N. moss4*, *N. moss5,* and *N. sp. 996*, six MAGs from our metagenomic assembly labeled bin14, bin192, bin238, bin354, bin377, and bin384, three binned genomes from the SPRUCE site, but outside the enclosures labeled bin109, bin297, and bin367, and one newly sequenced genome for *Nostoc muscorum*. A concatenated alignment of inferred amino acids sequences from 31 proteins for the 125 cyanobacterial genomes

was generated and trimmed using the AMPORA2 pipeline (Wu & Scott, 2012). Alignment sites containing only gaps and ambiguous characters were removed using FAST v1.6. Molecular evolution model selection was performed with ModelFinder (Kalyaanamoorthy *et al.*, 2017). Phylogenetic analysis was conducted with IQ-TREE v1.6.8 (Minh *et al.*, 2013) using the cpREV+C60+F+R6 model. Node support was evaluated using 1000 SH-like approximate likelihood ratio test replicates and 1000 UFboot2 replicates (Minh *et al.,* 2013).

References:

Buchfink B, Xie C, Huson DH. **2014**. Fast and sensitive protein alignment using DIAMOND. *Nature Methods* **12**: 59–60.

Carrell AA, Frank AC. **2014**. Pinus flexilis and Picea engelmannii share a simple and consistent needle endophyte microbiota with a potential role in nitrogen fixation. *Frontiers in Microbiology* **5**: 1–11.

Didion JP, Martin M, Collins FS. **2017**. Atropos: Specific, sensitive, and speedy trimming of sequencing reads. *PeerJ* **2017**: 1–19.

Hyatt D, Chen G-L, Locascio PF, Land ML, Larimer FW, Hauser LJ. **2010**. Prodigal: prokaryotic gene recognition and translation initiation site identification. *BMC Bioinformatics* **11**: 119.

Kalyaanamoorthy S, Minh BQ, Wong TKF, Von Haeseler A, Jermiin LS. **2017**. ModelFinder: Fast model selection for accurate phylogenetic estimates. *Nature Methods* **14**: 587–589.

Kang DD, Li F, Kirton E, Thomas A, Egan R, An H, Wang Z. **2019**. MetaBAT 2: an adaptive binning algorithm for robust and efficient genome reconstruction from metagenome assemblies. *PeerJ* **7**: e7359.

Li H, Durbin R. **2009**. Fast and accurate short read alignment with Burrows-Wheeler transform. **25**: 1754–1760.

Li D, Liu CM, Luo R, Sadakane K, Lam TW. **2015**. MEGAHIT: An ultra-fast single-node solution for large and complex metagenomics assembly via succinct de Bruijn graph. *Bioinformatics* **31**: 1674–1676.

Li D, Luo R, Liu CM, Leung CM, Ting HF, Sadakane K, Yamashita H, Lam TW. **2016**. MEGAHIT v1.0: A fast and scalable metagenome assembler driven by advanced methodologies and community practices. *Methods* **102**: 3–11.

Minh BQ, Anh M, Nguyen T, Von Haeseler A. **2013.** Ultrafast approximation for phylogenetic bootstrap. *Molecular Biology and Evolution* **30**:1188-95.

Parks DH, Imelfort M, Skennerton CT, Hugenholtz P, Tyson GW. **2015**. CheckM: Assessing the quality of microbial genomes recovered from isolates, single cells, and metagenomes. *Genome Research* **25**: 1043–1055.

Seemann T. **2014**. Genome analysis Prokka: rapid prokaryotic genome annotation. **30**: 2068–2069.

Shih PM, Wu D, Latifi A, Axen SD, Fewer DP, Talla E, Calteau A, Cai F, Tandeau De Marsac N, Rippka R, et al. 2013. Improving the coverage of the cyanobacterial phylum using diversity-driven genome sequencing. *Proceedings of the National Academy of Sciences of the United States of America* **110**: 1053–1058.

Warshan D, Espinoza JL, Stuart RK, Richter RA, Kim S-Y, Shapiro N, Woyke T, C Kyrpides N, Barry K, Singan V, et al. 2017. Feathermoss and epiphytic Nostoc cooperate differently: expanding the spectrum of plant–cyanobacteria symbiosis. *The ISME Journal* **11**: 2821–2833.

Wu M, Scott AJ. **2012**. Phylogenomic analysis of bacterial and archaeal sequences with AMPHORA2. *Bioinformatics Application Note* **28**: 1033–1034.

Available as separate files:

SI Dataset S1 (SI_dataset.xlsx)

Significantly enriched MapMan4 gene ontologies for Sphagnum mapped metatranscriptome reads. Statistical significance (padj) of ontology bins was determined using Kruskal–Wallis test with multiple testing correction performed using FDR. Average log2 fold change (avg_lfc) of MapMan4 bins was determined by averaging log2 fold change across differentially expressed genes. Up/down indicates the number of genes within the bin significantly upregulated (left of slash) and downregulated (right of slash). Differential gene expression was determined using limma-voom and considered significant if the FDR corrected p-value was <=0.05. Remaining abbreviation defined in Table S7.

SI Dataset S2 (SI_dataset.xlsx)

Significantly enriched SEED gene ontologies for microbial mapped metatranscriptome reads. Statistical significance (padj) was determined using Kruskal–Wallis test with multiple testing correction performed using FDR. Average log2 fold change (avg_lfc) was determined by averaging log2 fold change across differentially expressed genes. Differential gene expression was determined using limma-voom and considered significant if the FDR corrected p-value was <=0.05.